Published in final edited form as:
Invest Ophthalmol Vis Sci. 2006 March ; 47(3): 1069–1075.

A Novel αB-Crystallin Mutation Associated with Autosomal Dominant Congenital Lamellar Cataract

Yizhi Liu[1,2], **Xinyu Zhang**[1,2,3], **Lixia Luo**[1], **Mingxing Wu**[1], **Ruiping Zeng**[4], **Gang Cheng**[5], **Bin Hu**[5], **Bingfen Liu**[6], **Jack J. Liang**[6], and **Fu Shang**[3]

1*Zhongshan Ophthalmic Center, Sun Yat-sen University, Guangzhou, China*

3*Laboratory for Nutrition and Vision Research, USDA Human Nutrition Research Center on Aging, Tufts University, Boston, Massachusetts*

4*Medical Genetic Department, Sun Yat-sen University, Guangzhou, China*

5*Daan Gene Diagnosis Center, Sun Yat-sen University, Guangzhou, China*

6*Center for Ophthalmic Research, Brigham and Women's Hospital, Harvard Medical School, Boston, Massachusetts*

Abstract

Purpose—To identify the mutation and the underlying mechanism of cataractogenesis in a five-generation autosomal dominant congenital lamellar cataract family.

Methods—Nineteen mutation hot spots associated with autosomal dominant congenital cataract have been screened by PCR-based DNA sequencing. Recombinant wild-type and mutant human αB-crystallin were expressed in *Escherichia coli* and purified to homogeneity. The recombinant proteins were characterized by far UV circular dichroism, intrinsic tryptophan fluorescence, Bis-ANS fluorescence, multiangle light-scattering, and the measurement of chaperone activity.

Results—A novel missense mutation in the third exon of the αB-crystallin gene (*CRYAB*) was found to cosegregate with the disease phenotype in a five-generation autosomal dominant congenital lamellar cataract family. The single-base substitution (G→A) results in the replacement of the aspartic acid residue by asparagine at codon 140. Far UV circular dichroism spectra indicated that the mutation did not significantly alter the secondary structure. However, intrinsic tryptophan fluorescence spectra and Bis-ANS fluorescence spectra indicated that the mutation resulted in alterations in tertiary and/or quaternary structures and surface hydrophobicity of αB-crystallin. Multiangle light-scattering measurement showed that the mutant αB-crystallin tended to aggregate into a larger complex than did the wild-type. The mutant αB-crystallin was more susceptible than wild-type to thermal denaturation. Furthermore, the mutant αB-crystallin not only lost its chaperone-like activity, it also behaved as a dominant negative which inhibited the chaperone-like activity of wild-type αB-crystallin.

Conclusions—These data indicate that the altered tertiary and/or quaternary structures and the dominant negative effect of D140N mutant αB-crystallin underlie the molecular mechanism of cataractogenesis of this pedigree.

Congenital cataract is a common major abnormality of the eye, which frequently causes blindness in children. It is clinically and genetically heterogeneous, and the phenotype varies

Corresponding author: Fu Shang, Jean Mayer USDA Human Nutrition Research Center on Aging, Tufts University, 711 Washington Street, Boston, MA 02111; fu.shang@tufts.edu.

[2]Contributed equally to the work and therefore should be considered equivalent authors.

Disclosure: **Y. Liu**, None; **X. Zhang**, None; **L. Luo**, None; **M. Wu**, None; **R. Zeng**, None; **G. Cheng**, None; **B. Hu**, None; **B. Liu**, None; **J.J. Liang**, None; **F. Shang**, None

considerably between and within families.[1] It is most commonly inherited in an autosomal dominant manner, although recessive and X-linked forms also exist.[2–4] Congenital cataract may be isolated, be associated with other ocular developmental abnormality, or be a part of systemic disease. To date, mutations in dozens of genes have been described in association with isolated congenital cataract, including members of the crystallin and connexin families,[5] membrane proteins MIP[6] and LIM2,[2] cytoskeletal protein BFSP2,[7,8] and transcription factors PITX3[9] and HSF4.[10]

Crystallins account for nearly 90% of total lens protein and, not surprisingly, mutations in the crystallin genes represent a large proportion of the mutations identified in autosomal dominant congenital cataract (ADCC). These include αA-crystallin (*CRYAA*).[2,11] αB-crystallin (*CRYAB*),[12] βA1/A3-crystallin (*CRYBA1/A3*),[13,14] βB1-crystallin (*CRYBB1*),[15] βB2-crystallin (*CRYBB2*),[16,17] γC-crystallin (*CRYGC*),[18,19] and γD-crystallin (*CRYGD*) mutations.[18,20] Among the lens crystallins, α-crystallin is considered to play an important role in maintaining the transparency of the lens. α-Crystallins are members of the highly conserved small heat shock protein (sHsp) family. A typical mammalian lens contains approximately 35% α-crystallin, which makes it one of the major protein components that produce the necessary refractive index. α-Crystallin in the lens exists as hetero-oligomers composed of two components, αA- and αB-crystallin. The subunits of αA- and αB-crystallin have molecular masses of ~20 kDa with approximately 57% amino-acid sequence homology. The ratio of αA to αB in the lens is generally 3:1. In addition to being a major structural building block, α-crystallin, like other members of the sHsp family, has chaperone-like activity in preventing aggregation of other lens proteins induced by heat or other stressors.[21–24]

Two mutations in the *CRYAB* gene have been reported to be associated with cataract. A missense mutation R120G was associated with cataract and desmin-related myopathy,[25] and a deletion mutation, 450delA, was associated with isolated autosomal dominant posterior polar cataract.[12] In the present study, we report a novel D140N mutation in the *CRYAB* gene in an ADCC family with isolated lamellar cataract. To characterize the possible structural and functional changes that underlie the molecular mechanism of cataract caused by this mutation, we expressed the wild-type and the mutant αB-crystallin in vitro, and compared the secondary, tertiary, and quaternary structures as well as chaperone-like activity between the wild-type and mutant proteins.

Materials and Methods

Clinical Data and Sample Collection

The procurement of congenital cataract and genetic material from the ADCC-affected family was approved by the human research ethics committees of Zhongshan Ophthalmic Center, and Sun yat-sen University (Guangzhou, China), and informed consent was obtained from all participants or their guardians. The research followed the tenets of the Declaration of Helsinki. A five-generation Chinese ADCC family was referred to Zhongshan Ophthalmic Center. Nine members of the family, including four with congenital cataract and five unaffected relatives, underwent full ophthalmic examinations including visual acuity, slit lamp microscopy, fundus examination with dilated pupil, intraocular pressure, and B-ultrasonic scanning. The status of other patients in the family was obtained by family history and accessing the patients' medical records. One hundred unaffected, unrelated individuals who came in for routine physical checkups were enrolled in the study and underwent the same ophthalmic examination with informed consent. Blood samples were obtained from a peripheral vein, and genomic DNA was extracted (QIAmp Blood kit; Qiagen, Valencia, CA).

Mutation Analysis

To identify the mutation that causes cataract in this pedigree, 19 mutation hot spots were screened in all nine recruited family members by polymerase chain reaction (PCR) of the 10 involved gene segments and direct sequencing of the PCR product. To exclude the possibility that polymorphism may account for the novel mutation in *CRYAB*, the *CRYAB* gene fragment of 100 unrelated normal individuals was sequenced. These mutation hot spots included *CRYAA* (R116C),[11] *CRYAB* (DEL450A, R120G),[12,25] *CRYBA1* (EX3-4 DEL),[13] *CRYBB2* (Q155TER),[16] *CRYGC* (T5P′5-BP DUP at NT226),[18] *CRYGD* (R14C′P23T′R58H′R36S),[18–20,26] GJA3 (N63S′P187L),[27,28] GJA8 (E48K′P88S,29,[30] BFSP2 (R287W, DeltaE233)[7,8] and MIP (E134G′T138R),[6] which have been identified as causes of ADCC. Primers to amplify the gene segments were designed from the published partial genomic sequence and the full-length cDNA sequence and synthesized by Daan Genetic Diagnostic Center (Guangzhou, China). The primers used, their locations in the genomic sequence, and annealing temperatures are summarized in Supplementary Table S1, online at http://www.iovs.org/cgi/content/full/47/3/1069/DC1. A sample of 100 ng human genomic DNA was used for PCRs with 2.5 pM primer in a 50-μL reaction mixture. PCR was performed in a thermocycler (PE9600; Applied Biosystems [ABI] Foster City, CA). PCR conditions were as follows: predenaturing at 94°C for 7 minutes, followed by 35 cycles of denaturing at 94°C for 1 minute, annealing at 57 to 62°C for 1 minute, and extension at 72°C for 1 minute.

PCR products were analyzed on 1% agarose gels and purified (QIAquick Gel Extraction Kit; Qiagen) followed by ethanol–sodium acetate precipitation. Sequencing in the forward and reverse directions with the gene-specific primers was then performed (model 3100 Prism automated sequencer; ABI, by using an Ampli*Taq* FS cycle sequencing kit with dye-labeled terminators [both from ABI]). Sequences of the 10 gene segments were compared with those published in GenBank (http://www.ncbi.nlm.nih.gov/genbank; provided in the public domain by the National Center for Biotechnology Information, Bethesda, MD). When ambiguous sequences (heterozygous) were detected, the PCR products were cloned into a pCR-TOPO vector (Invitrogen, Carlsbad, CA), and the sequences were confirmed by sequencing the cloned products.

Site-Directed Mutagenesis

To express the recombinant mutant αB-crystallin, the cDNA of human αB-crystallin was mutated by PCR-based, site-directed mutagenesis. The αB mutant in which aspartic acid 140 was replaced by asparagine (D140N) was generated by GAT→AAT conversion at the 418th nucleotide of the *CRYAB* gene. The substitution was made by incorporating the mismatch in the PCR primer. Two pairs of primer were used in the mutagenesis, the sequences of which are as follows: CRBN forward (F), 5′-GACATCGCCATCCACCAC-3′, CRBN reverse (R), 5′-GACCCCATTAGATGACAG-3′; and CRBCF, 5′-CTGTCATCTAATGGGGTC-3′, CRBCR, 5′-CTATTTCTTGGGGGCTGC-3′.

Two rounds of PCR were used to create the mutation. The first round produced the N-terminal fragment with CRBNF/CRBNR as a pair of primers and the C-terminal fragment with CRBCF/CRBCR as a pair of primers. The second round of PCR used the mixture of the N-terminal and the C-terminal fragments as the template, and CRBNF/CRBCR as a pair of primers to generate the full-length mutant cDNA. PCR conditions were as followed: predenaturing at 94°C for 2 minutes, followed by 35 cycles of denaturing at 94°C for 15 seconds, annealing at 60°C for 40 seconds, and extension at 72°C for 40 seconds. PCR products were analyzed on a 1% agarose gel and purified (QIAquick Gel Extraction Kit; Qiagen).

Expression and Purification of Recombinant Wild-Type and D140N Mutant αB-Crystallins

Purified PCR product of the mutant *CRYAB* gene was cloned into the pET15b vector at the *Nco*I site (after fill-in with Klenow fragment) to generate the pET15b-D140NαB plasmid. The presence of the mutation and the absence of any other base change in the coding region of the αB-crystallin gene were confirmed by DNA sequencing. The expression plasmid pET15b-wtαB and pET15b-D140NαB were transformed into competent *Escherichia coli* BL21 (DE3) cells. Growth, induction, and lysis of cells and purification of the recombinant proteins were performed essentially as described previously.[21,23] Protein concentrations were determined by measuring absorption at 280 nm with the absorbance $A^{0.1\%} = 0.742$ for both wild-type and mutant, calculated based on the amount of aromatic amino acids.[31] Wild-type and mutant proteins were analyzed on 15% SDS-polyacrylamide gels under reducing conditions and stained with Coomassie brilliant blue R250 (Sigma-Aldrich, St. Louis, MO). The recombinant proteins were electrotransferred to a nitrocellulose membrane. The primary antibody for αB-crystallin was raised in rabbit and the secondary antibody was anti-rabbit IgG alkaline phosphatase conjugates (Roche Molecular Biochemicals, Indianapolis, IN). To determine the sizes of oligomers of wild-type and mutant αB crystallins, we analyzed the αB crystallin solutions by HPLC size-exclusion chromatography (Shodex protein KW-803) coupled with a three-angle (45°, 90 °, and 135°) light-scattering detector coupled with an interferometric refractometer (Wyatt Technology, Santa Barbara, CA). The mobile phase was 25 mM Tris (pH 7.5), 100 mM NaCl, 1 mM dithiothreitol (DTT), and 1 mM EDTA. The flow rate was 0.5 mL/min.

Study of Conformational Change

Size-exclusion chromatography was performed (a Fast Protein Liquid Chromatography [FPLC] system equipped with FPLC director software and a superose-12 column; GE Healthcare, Piscataway, NJ). Circular dichroic (CD) spectra were obtained with a circular dichroism spectrometer (model 60 DS; Aviv Associates, Lakewood, NJ). Five scans were recorded and averaged, followed by a polynomial fitting program. The CD was expressed in deg-cm^2/dmol. Fluorescence was measured with a spectrofluorometer (model RF-5301PC; Shimadzu Instruments, Columbia, MD). Tryptophan fluorescence emission was scanned with an excitation wavelength of 295 nm. Bis-ANS fluorescence emission spectra were scanned between 460 and 560 nm with an excitation wavelength of 395 nm. Aliquots of 50 μL of Bis-ANS (5.5×10^{-5} M stock solution) were added to 1 mL of αB-crystallin solution (0.1 mg/mL in 50 mM phosphate buffer; pH7.5) until saturation was reached. The samples were incubated for 10 minutes at room temperature before fluorescence measurement.

Chaperone-like Activity Measurement

Chaperone-like activity of the wild-type and mutant proteins was studied by the insulin aggregation assay. The aggregation of insulin (0.2 mg/mL) in 10 mM phosphate buffer (pH 7.4), containing 100 mM NaCl, was initiated by the addition of 25 μL of 1 M DTT to 240 μL of insulin at room temperature. The extent of aggregation was measured as a function of time by monitoring light scattering at 405 nm in a plate reader (Spectra MAX-340; Molecular Devices, Sunnyvale, CA). The extent of protection by the wild-type and mutant αB-crystallin was studied by incubating insulin with required concentrations of αB-crystallin sample for 10 minutes at room temperature before addition of DTT.

Thermal Stability Measurements

Thermal stability was studied by time-dependent change in light scattering at 360 nm of both wild-type and D140N mutant proteins at 65°C. The light scattering was measured using a UV-visible spectrophotometer (BioSpec-1601; Shimadzu).

Results

Clinical Findings

Members of a five-generation family (Fig. 1) from South China and 100 unaffected, unrelated individuals were invited to take part in this study. All available affected individuals displayed bilateral lamellar cataracts (Fig. 2) with variable severity and without other ocular or systemic abnormalities. The cataracts in this family were inherited in an autosomal dominant manner. The clinical details are summarized in Table 1.

Mutation Analysis

To identify the mutation that causes cataract in this pedigree, we screened 19 mutation hot spots of 10 genes in all nine recruited family members by PCR-based DNA sequencing. None of these mutation hot spots was associated with this pedigree. However, sequencing the *CRYAB* gene segment revealed a novel G→A mutation in the third exon of the gene in all four affected members of this family (Fig. 3). This single-base substitution resulted in the replacement of the aspartic acid residue by asparagine at codon 140 (D140N). The sequence change was not found in the 5 unaffected members of the family, nor in the 100 unaffected, unrelated, normal individuals. This indicates that the single-base substitution, rather than a rare polymorphism, is the cause of cataract in this pedigree.

Expression and Purification of Wild-Type and D140N Mutant αB-Crystallin

To investigate the molecular mechanisms that underlie the cataractogenesis of this mutation, wild-type and D140N mutant αB-crystallin proteins were expressed in *E. coli* BL21 (DE3). The D140N mutant αB-crystallin cDNA was generated by PCR-based, site-directed mutation. The expression of recombinant proteins was monitored by SDS-PAGE and Western blot analysis. Whereas wild-type protein was mainly in the water-soluble fraction, 20% to 50% of the D140N mutant αB-crystallin was found in the water-insoluble fraction (data not shown). The wild-type and mutant αB-crystallins were purified from the water-soluble fraction by anion exchange and size-exclusion chromatography to near homogeneity (95%). As shown in Figure 4A, the purified protein migrated as a single 20-kDa band on SDS-PAGE, which was recognized by antibodies to αB-crystallin (Fig. 4B). αB-crystallin exists as noncovalently linked oligomers with an apparent molecular mass of ~570 kDa in native state.[32] The retention times of wild-type and mutant αB-crystallins were not distinguishable on size-exclusion FPLC. However, multiangle light-scattering measurement showed that the sizes of mutant αB-crystallin oligomers were larger than those of wild-type. The average mass of wild-type αB-crystallin was 5.692×10^5 (3×10^5 to 9×10^5) and the average mass of D140N mutant αB-crystallin was 7.938×10^5 (1×10^5 to 4×10^6; Fig. 5). The data show that sizes of oligomers of mutant αB-crystallin were not only larger, but more heterogeneous than those of wild-type αB-crystallin.

Surface Hydrophobicity

The difference in sizes and in solubility of the mutant αB-crystallin in native state from those of wild-type suggests that the mutant αB-crystallin adapts a different conformation. To test this possibility, we compared the surface hydrophobicity of wild-type and the mutant αB-crystallins. The surface hydrophobicity was determined by Bis-ANS fluorescence. Bis-ANS (a hydrophobic probe) is nonfluorescent in aqueous solution and becomes fluorescent when bound to the hydrophobic residues on the surface of a molecule. Figure 6 shows the fluorescence intensity of wild-type and D140N mutant αB-crystallins after binding with Bis-ANS at room temperature. The fluorescence intensity was much higher in mutant protein than in the native one, which suggests an increase in hydrophobicity of the mutant protein due to exposure of normally buried hydrophobic residues.

Secondary and Tertiary Structure Analyses

Comparative analyses of secondary and tertiary structure of wild-type and mutant αB-crystallin were performed by determining their CD spectra and tryptophan fluorescence, respectively. The far UV CD spectrum reflects the secondary structure. As shown in Figure 7A, there was no significant difference in the far UV CD spectra of wild-type and D140N mutant αB-crystallins, indicating that wild-type and mutant αB-crystallins share a similar, if not identical, secondary structure. Tryptophan fluorescence data reflect a protein's gross positioning of tryptophan residues, which normally reflects the tertiary and/or quaternary structures of a protein. Improperly folded or partially unfolded proteins usually have altered tryptophan fluorescence intensity and a shift of the wavelength of fluorescence emission maxima.[33] We found that the D140N mutant showed higher fluorescence intensity and a shift emission maximum from 340 nm to 345 nm (Fig. 7B), indicating a significant change in the local environment of tryptophan residues compared with the wild-type protein, and indicating that the mutant αB-crystallin adapted different tertiary and/or quaternary structures from that of wild type.

Thermal Stability and Chaperone-like Activity

αB-crystallin belongs to the small heat shock protein family. Wild-type crystallins are normally thermally stable, and they can prevent heat-induced aggregation and precipitation of other proteins.[22] To determine further the molecular mechanism by which the mutation causes cataract, we compared the thermal stability and chaperone activity of wild-type and D140N mutant αB-crystallins. As shown in Figure 8, the D140N mutant αB-crystallin was susceptible to heat-induced aggregation. When incubated at 65°C, wild-type αB-crystallin remained soluble for at least 120 minutes, whereas the mutant αB-crystallin aggregated within 15 minutes. Wild-type αB-crystallin can prevent heat-induced aggregation of many other proteins,[34] but it could not prevent thermal-induced aggregation of the mutant αB-crystallin (Fig. 8). Because the mutant αB-crystallin was not thermally stable, we chose DTT-reduced insulin as a substrate for the chaperone activity. When incubated at a 1:1 (wt/wt) ratio, wild-type αB-crystallin significantly inhibited DTT-induced aggregation of insulin (Fig. 9A). However, the same amount of D140N mutant αB-crystallin could not prevent the aggregation of insulin. In contrast, the mutant αB-crystallin enhanced the DTT-induced aggregation of insulin (Fig. 9A). Moreover, the chaperone-like activity of wild-type αB-crystallin was compromised when D140N mutant αB-crystallin was added (Fig. 9B). These data indicate that the mutant αB-crystallin behaves as a dominant negative, which interferes with the chaperone activity of wild-type αB-crystallin.

Discussion

We report a novel G→A mutation in the third exon of the *CRYAB* gene that is associated with cataractogenesis in an ADCC family. The data indicate that D140N is the causative mutation in this ADCC family, rather than a rare polymorphism in the normal population. First, the mutation cosegregated with the disease phenotype in the family and was absent in 100 unaffected, unrelated individuals screened. Second, the mutation resulted in a substitution of a negative charged aspartic acid by a neutral asparagine residue at codon 140 within the highly conserved α-crystallin domain. Third, the recombinant mutant αB-crystallin showed abnormal oligomerization, reduced thermal stability, and abolished chaperone-like activity. Furthermore, the D140N mutant αB-crystallin behaves as a dominant negative, which interferes with the chaperone-like activity of wild-type αB-crystallin. The reduced thermal stability and the dominant negative effects of the mutant αB-crystallin may be the direct cause of cataract, because αB-crystallin-null mice have clear lenses.[35]

Like most sHsps, αB-crystallin contains a highly conserved sequence of 80 to 100 amino residues called the α-crystallin domain. The crystal structure of α-crystallin is not available currently. Based on the sequence homology to other members of the sHsp family, it is proposed that this domain forms a variant of the seven-β-strand Ig-like fold.[36–38] There are regions in this domain that have been shown to bind substrate protein such as alcohol dehydrogenase and the hydrophobic probe bis-ANS. This domain is also known to be involved in intersubunit contacts.[39,40] Mutations in this domain, such as the D140N mutation that we report herein, would have functional consequences. Consistent with this idea, several mutations in this region, such as R49C,[41] R54H,[42] and R116C[11] mutations in αA-crystallin and the R120G mutation[25] or a frame-shift mutation[12] in αB-crystallin, are associated with congenital cataract.

Tryptophan fluorescence revealed that D140N mutation leads to an alteration in tertiary or quaternary structures. This structural change is further supported by the increased surface hydrophobicity and decreased thermal stability. This change is further corroborated in alteration of oligomerization status, such as an appreciable increase in the sizes of oligomers of the mutant αB-crystallin. The structural and functional changes associated with the D140N mutation of αB-crystallin are similar, but not identical, to those of R120G or N146D mutant αB-crystallin.[32,43,44] Similar to the D140N mutant αB-crystallin reported herein, both R120G and N146D mutant αB-crystallins showed increased hydrophobicity, abnormal oligomerization, and reduced chaperone activity.[32,43,44] However, unlike the D140N mutant αB-crystallin which has a similar, if not identical, secondary structure as wild-type αB-crystallin, R120G mutation causes alteration in the secondary structure.[43,44]

It is interesting to note that the aspartic acid residue at position 140 is conserved in different species of mammals and other vertebrates, such as rabbit, bovine, rat, hamster, mouse, chicken, mallard-duck, bullfrog, and catfish.[45] The highly conserved nature of this residue indicates its important role in maintaining the structure and functions of αB-crystallin. It has been reported that maintenance of the net charge is critical for the chaperone activity of α-crystallins. Site-directed mutation studies have revealed that chaperone-like activity of α-crystallins would be compromised whenever charged residues are mutated.[34,46] Although the R120 and D140 residues are not directly involved in the subunit–subunit interaction,[40] R120G and D140N mutations resulted in abnormal oligomerization. It is therefore likely that both R120 and D140 residues are necessary for maintaining the structure of αB-crystallin for proper subunit–subunit interactions. This critical requirement may explain why the D140 residue of α-crystallins was conserved through evolution.[47] Together with previously published data, the present study indicates that disturbing the net charge of the αB-crystallin will alter the tertiary and/or quaternary structures, reduce or abolish the chaperone activity, and cause severe physiological consequences, such as congenital cataract.

It is worth noting that although both R120G and D140N mutations results in similar structure changes, the D140N mutation causes isolated cataract phenotype whereas the R120G mutation causes myopathy as well as cataract. We speculate that the dominant negative effect of the D140N mutation is one of the major mechanisms of the cataract phenotype. In most cases, dominant negative is dose dependent. Although αB-crystallin is expressed in other tissues, particularly in muscles, the expression levels in these tissues are much lower than the expression in lens and it may not reach the levels that are necessary for inhibiting the chaperone activity of wild-type αB-crystallin or other sHsps. Another possibility is that the mutant αB-crystallin was rapidly degraded in muscles, which have active proteolytic systems. A comparison of the susceptibilities of R120G αB-crystallin and D140N αB-crystallin to proteolytic degradation could provide an explanation for the different phenotypes between R120G mutation and D140N mutation. This difference will be evaluated in the future.

Supplementary Material

Refer to Web version on PubMed Central for supplementary material.

Acknowledgements

The authors thank the family and all subjects for taking part in this study.

References

1. Ionides A, Francis P, Berry V, et al. Clinical and genetic heterogeneity in autosomal dominant cataract. Br J Ophthalmol 1999;83:802–808. [PubMed: 10381667]
2. Pras E, Frydman M, Levy-Nissenbaum E, et al. A nonsense mutation (W9X) in CRYAA causes autosomal recessive cataract in an inbred Jewish Persian family. Invest Ophthalmol Vis Sci 2000;41:3511–3515. [PubMed: 11006246]
3. Kramer PL, LaMorticella D, Schilling K, et al. A new locus for autosomal dominant congenital cataracts maps to chromosome 3. Invest Ophthalmol Vis Sci 2000;41:36–39. [PubMed: 10634598]
4. Reddy MA, Francis PJ, Berry V, Bhattacharya SS, Moore AT. Molecular genetic basis of inherited cataract and associated phenotypes. Surv Ophthalmol 2004;49:300–315. [PubMed: 15110667]
5. Francis PJ, Berry V, Moore AT, Bhattacharya S. Lens biology: development and human cataractogenesis. Trends Genet 1999;15:191–196. [PubMed: 10322486]
6. Berry V, Francis P, Kaushal S, Moore A, Bhattacharya S. Missense mutations in MIP underlie autosomal dominant 'polymorphic' and lamellar cataracts linked to 12q. Nat Genet 2000;25:15–17. [PubMed: 10802646]
7. Conley YP, Erturk D, Keverline A, et al. A juvenile-onset, progressive cataract locus on chromosome 3q21–q22 is associated with a missense mutation in the beaded filament structural protein-2. Am J Hum Genet 2000;66:1426–1431. [PubMed: 10729115]
8. Jakobs PM, Hess JF, FitzGerald PG, et al. Autosomal-dominant congenital cataract associated with a deletion mutation in the human beaded filament protein gene BFSP2. Am J Hum Genet 2000;66:1432–1436. [PubMed: 10739768]
9. Semina EV, Ferrell RE, Mintz-Hittner HA, et al. A novel homeobox gene PITX3 is mutated in families with autosomal-dominant cataracts and ASMD. Nat Genet 1998;19:167–170. [PubMed: 9620774]
10. Bu L, Jin Y, Shi Y, et al. Mutant DNA-binding domain of HSF4 is associated with autosomal dominant lamellar and Marner cataract. Nat Genet 2002;31:276–278. [PubMed: 12089525]
11. Litt M, Kramer P, LaMorticella DM, et al. Autosomal dominant congenital cataract associated with a missense mutation in the human alpha crystallin gene CRYAA. Hum Mol Genet 1998;7:471–474. [PubMed: 9467006]
12. Berry V, Francis P, Reddy MA, et al. Alpha-B crystallin gene (CRYAB) mutation causes dominant congenital posterior polar cataract in humans. Am J Hum Genet 2001;69:1141–1145. [PubMed: 11577372]
13. Kannabiran C, Rogan PK, Olmos L, et al. Autosomal dominant zonular cataract with sutural opacities is associated with a splice mutation in the betaA3/A1-crystallin gene. Mol Vis 1998;4:21. [PubMed: 9788845]
14. Bateman JB, Geyer DD, Flodman P, et al. A new betaA1-crystallin splice junction mutation in autosomal dominant cataract. Invest Ophthalmol Vis Sci 2000;41:3278–3285. [PubMed: 11006214]
15. Mackay DS, Boskovska OB, Knopf HL, Lampi KJ, Shiels A. A nonsense mutation in CRYBB1 associated with autosomal dominant cataract linked to human chromosome 22q. Am J Hum Genet 2002;71:1216–1221. [PubMed: 12360425]
16. Litt M, Carrero-Valenzuela R, LaMorticella DM, et al. Autosomal dominant cerulean cataract is associated with a chain termination mutation in the human beta-crystallin gene CRYBB2. Hum Mol Genet 1997;6:665–668. [PubMed: 9158139]
17. Gill D, Klose R, Munier FL, et al. Genetic heterogeneity of the Coppock-like cataract: a mutation in CRYBB2 on chromosome 22q11.2. Invest Ophthalmol Vis Sci 2000;41:159–165. [PubMed: 10634616]

18. Heon E, Priston M, Schorderet DF, et al. The gamma-crystallins and human cataracts: a puzzle made clearer. Am J Hum Genet 1999;65:1261–1267. [PubMed: 10521291]
19. Ren Z, Li A, Shastry BS, et al. A 5-base insertion in the gammaC-crystallin gene is associated with autosomal dominant variable zonular pulverulent cataract. Hum Genet 2000;106:531–537. [PubMed: 10914683]
20. Stephan DA, Gillanders E, Vanderveen D, et al. Progressive juvenile- onset punctate cataracts caused by mutation of the gammaD-crystallin gene. Proc Natl Acad Sci USA 1999;96:1008–1012. [PubMed: 9927684]
21. Horwitz J, Huang QL, Ding L, Bova MP. Lens alpha-crystallin: chaperone-like properties. Methods Enzymol 1998;290:365–383. [PubMed: 9534176]
22. Horwitz J. Alpha-crystallin can function as a molecular chaperone. Proc Natl Acad Sci USA 1992;89:10449–10453. [PubMed: 1438232]
23. Sun TX, Das BK, Liang JJ. Conformational and functional differences between recombinant human lens alphaA- and alphaB-crystallin. J Biol Chem 1997;272:6220–6225. [PubMed: 9045637]
24. Augusteyn RC. alpha-Crystallin: a review of its structure and function. Clin Exp Optom 2004;87:356–366. [PubMed: 15575808]
25. Vicart P, Caron A, Guicheney P, et al. A missense mutation in the alphaB-crystallin chaperone gene causes a desmin-related myopathy. Nat Genet 1998;20:92–95. [PubMed: 9731540]
26. Kmoch S, Brynda J, Asfaw B, et al. Link between a novel human gammaD-crystallin allele and a unique cataract phenotype explained by protein crystallography. Hum Mol Genet 2000;9:1779–1786. [PubMed: 10915766]
27. Mackay D, Ionides A, Kibar Z, et al. Connexin46 mutations in autosomal dominant congenital cataract. Am J Hum Genet 1999;64:1357–1364. [PubMed: 10205266]
28. Rees MI, Watts P, Fenton I, et al. Further evidence of autosomal dominant congenital zonular pulverulent cataracts linked to 13q11 (CZP3) and a novel mutation in connexin 46 (GJA3). Hum Genet 2000;106:206–209. [PubMed: 10746562]
29. Berry V, Mackay D, Khaliq S, et al. Connexin 50 mutation in a family with congenital “zonular nuclear” pulverulent cataract of Pakistani origin. Hum Genet 1999;105:168–170. [PubMed: 10480374]
30. Shiels A, Mackay D, Ionides A, et al. A missense mutation in the human connexin50 gene (GJA8) underlies autosomal dominant “zonular pulverulent” cataract, on chromosome 1q. Am J Hum Genet 1998;62:526–532. [PubMed: 9497259]
31. Mach H, Middaugh CR, Lewis RV. Statistical determination of the average values of the extinction coefficients of tryptophan and tyrosine in native proteins. Anal Biochem 1992;200:74–80. [PubMed: 1595904]
32. Gupta R, Srivastava OP. Effect of deamidation of asparagine 146 on functional and structural properties of human lens alphaB-crystallin. Invest Ophthalmol Vis Sci 2004;45:206–214. [PubMed: 14691175]
33. Kosinski-Collins MS, King J. In vitro unfolding, refolding, and polymerization of human gammaD crystallin, a protein involved in cataract formation. Protein Sci 2003;12:480–490. [PubMed: 12592018]
34. Plater ML, Goode D, Crabbe MJ. Effects of site-directed mutations on the chaperone-like activity of alphaB-crystallin. J Biol Chem 1996;271:28558–28566. [PubMed: 8910485]
35. Brady JP, Garland DL, Green DE, et al. αB-crystallin in lens development and muscle integrity: a gene knockout approach. Invest Ophthalmol Vis Sci 2001;42:2924–2934. [PubMed: 11687538]
36. Guruprasad K, Kumari K. Three-dimensional models corresponding to the C-terminal domain of human alphaA- and alphaB-crystallins based on the crystal structure of the small heat-shock protein HSP16.9 from wheat. Int J Biol Macromol 2003;33:107–112. [PubMed: 14599592]
37. Kim KK, Kim R, Kim SH. Crystal structure of a small heat-shock protein. Nature 1998;394:595–599. [PubMed: 9707123]
38. van Montfort RL, Basha E, Friedrich KL, Slingsby C, Vierling E. Crystal structure and assembly of a eukaryotic small heat shock protein. Nat Struct Biol 2001;8:1025–1030. [PubMed: 11702068]

39. Pasta SY, Raman B, Ramakrishna T, Rao Ch M. Role of the C-terminal extensions of alpha-crystallins: swapping the C-terminal extension of alpha-crystallin to alphaB-crystallin results in enhanced chaperone activity. J Biol Chem 2002;277:45821–45828. [PubMed: 12235146]
40. Ghosh JG, Clark JI. Insights into the domains required for dimerization and assembly of human alphaB crystallin. Protein Sci 2005;14:684–695. [PubMed: 15722445]
41. Mackay DS, Andley UP, Shiels A. Cell death triggered by a novel mutation in the alphaA-crystallin gene underlies autosomal dominant cataract linked to chromosome 21q. Eur J Hum Genet 2003;11:784–793. [PubMed: 14512969]
42. Chang B, Hawes NL, Roderick TH, et al. Identification of a missense mutation in the alphaA-crystallin gene of the lop18 mouse. Mol Vis 1999;5:21. [PubMed: 10493778]
43. Bova MP, Yaron O, Huang Q, et al. Mutation R120G in alphaB-crystallin, which is linked to a desmin-related myopathy, results in an irregular structure and defective chaperone-like function. Proc Natl Acad Sci USA 1999;96:6137–6142. [PubMed: 10339554]
44. Treweek TM, Rekas A, Lindner RA, et al. R120G alphaB-crystallin promotes the unfolding of reduced alpha-lactalbumin and is inherently unstable. FEBS J 2005;272:711–724. [PubMed: 15670152]
45. Avivi A, Joel A, Nevo E. The lens protein alpha-B-crystallin of the blind subterranean mole-rat: high homology with sighted mammals. Gene 2001;264:45–49. [PubMed: 11245977]
46. Smulders RH, Merck KB, Aendekerk J, et al. The mutation Asp69–>Ser affects the chaperone-like activity of alpha A-crystallin. Eur J Biochem 1995;232:834–838. [PubMed: 7588723]
47. de Jong WW, Zweers A, Versteeg M, Nuy-Terwindt EC. Primary structures of the alpha-crystallin A chains of twenty-eight mammalian species, chicken and frog. Eur J Biochem 1984;141:131–140. [PubMed: 6723655]

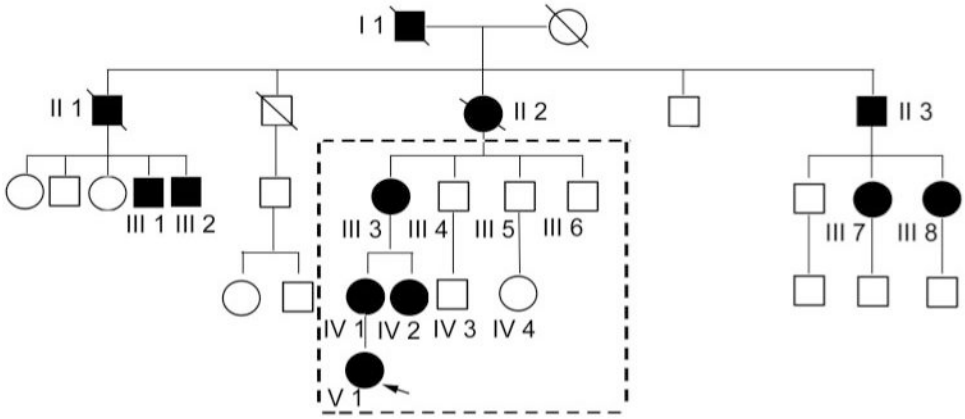

FIGURE 1.

The Chinese autosomal dominant congenital cataract pedigree. *Square symbols*: males; *round ones*: females; *shaded symbols*: ophthalmologist-confirmed congenital cataract; *arrow*: proband. Individuals in the *dashed box* were screened for mutations. The transmission pattern suggests the cataract is inherited in an autosomal dominant manner.

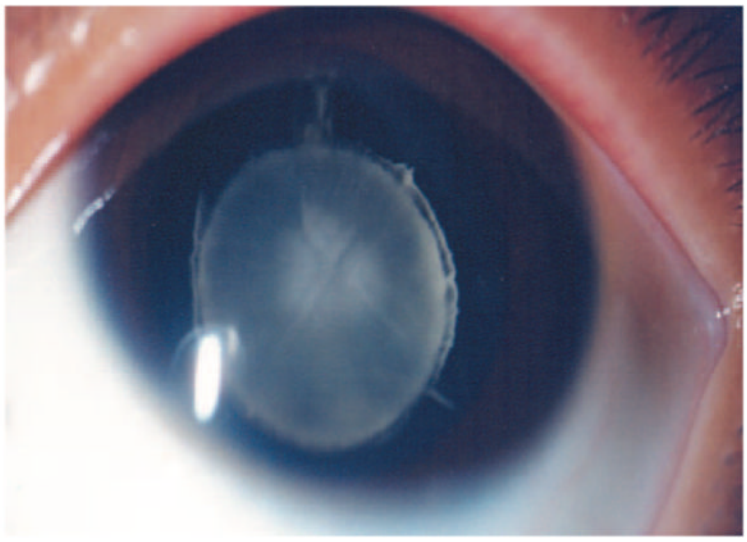

FIGURE 2.
Anterior segment photograph of the proband in the ADCC pedigree through slit lamp microscope. The opacification of the lens is restricted to discrete lamellae and the inner embryonic nucleus. The surrounding cortex remains clear.

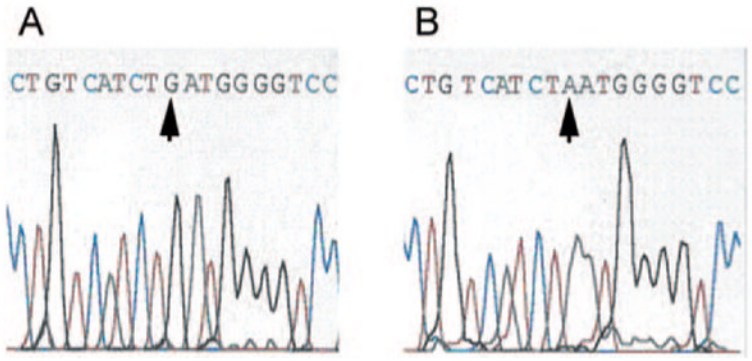

FIGURE 3.

Sequence analysis of the *CRYAB* gene in one unaffected (**A**) and one affected (**B**) individual of the ADCC family. *Arrow*: a G→A base change in the gene segment. The data show the sequences of representative clones of wild-type and mutant *CRYAB*.

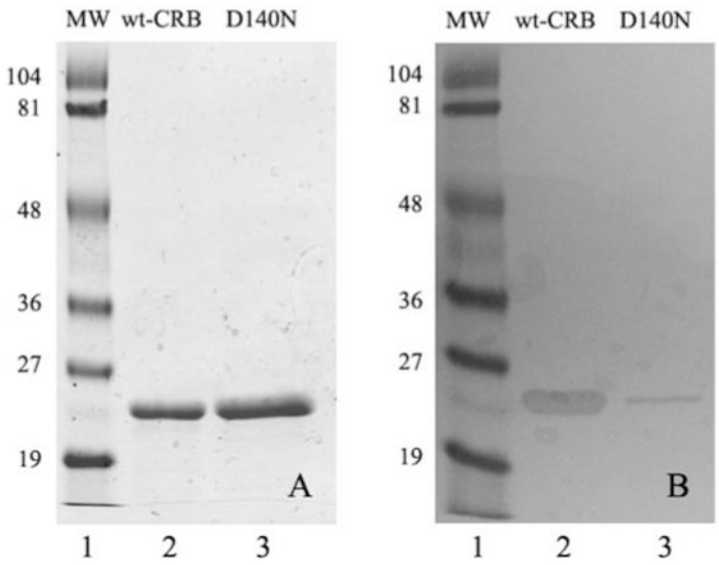

FIGURE 4.

SDS-PAGE and Western immunoblot analysis of wild-type and D140N mutant αB-crystallin. (**A**) Coomassie blue stain; (**B**) Western blot analysis. *Lane 1*: low-molecular-weight protein standards; *lane 2*: purified wild-type αB-crystallin; *lane 3*: purified D140N mutant αB-crystallin.

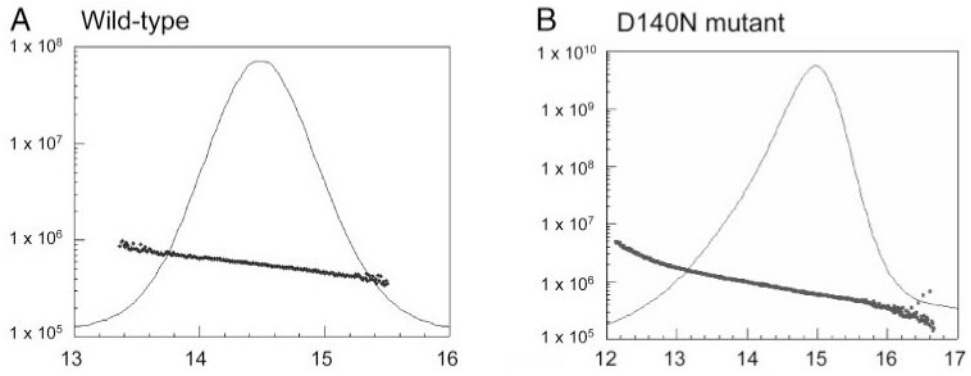

FIGURE 5.

Size-exclusion HPLC-multiangle light-scattering analysis of wild-type and D140N mutant αB-crystallins. (**A**) Wild-type αB-crystallin. The average mass was 5.692×10^5 Da, ranging from 3×10^5 to 9×10^5 Da. (**B**) D140N mutant αB-crystallin. The average mass was 7.938×10^5 Da, ranged from 1×10^5 to 4×10^6 Da.

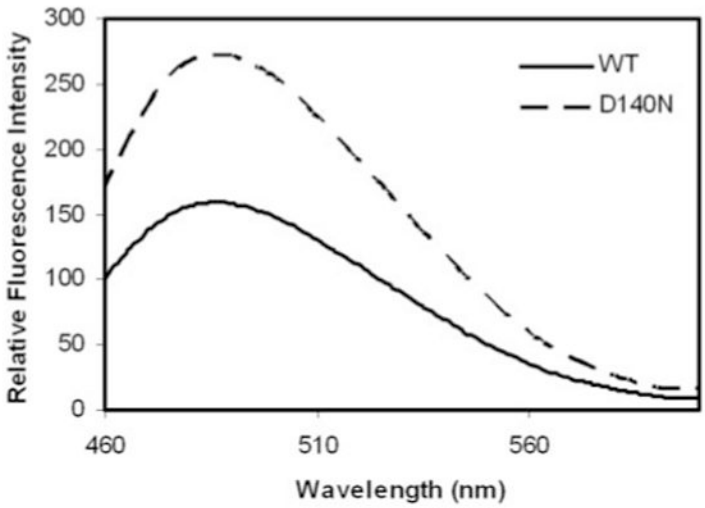

FIGURE 6.

Surface hydrophobicity of wild-type and D140N mutant αB-crystallins. Bis-ANS fluorescence of wild-type αB-crystallin (*solid line*) and D140N mutant αB-crystallin (*dashed line*) measured at room temperature. The fluorescence intensity was much higher in mutant than in native protein, indicating the increase in surface hydrophobicity.

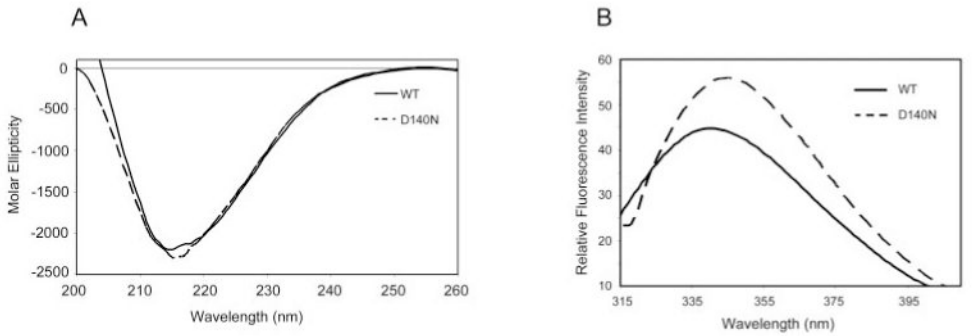

FIGURE 7.

CD and tryptophan fluorescence (**A**) shows far UV CD spectra of wild-type (*solid line*) and D140N mutant (*dashed line*) αB-crystallin. The lack of significant difference in CD spectra of wild-type and the mutant αB-crystallin suggests that the mutation did not cause detectable alterations in the secondary structure. (**B**) Tryptophan fluorescence spectra of wild-type (*solid line*) and D140N mutant (*dashed line*) αB-crystallin measured at room temperature. The fluorescence emission spectrum of wild-type had the λmax at 340 nm. The D140N mutant showed higher fluorescence intensity than wild-type and a shift of the λmax from 340 to 345 nm. The increased fluorescence intensity and the shift of the λmax of the mutant αB-crystallin indicate an alteration of the tertiary and/or quaternary structures.

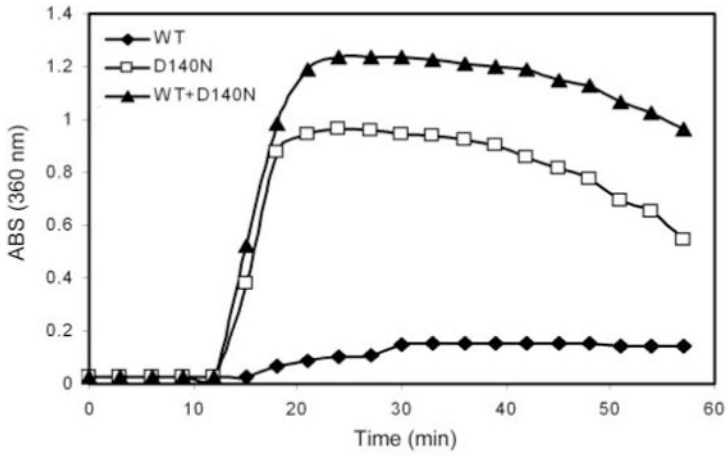

FIGURE 8.

Thermal stability of wild-type and mutant αB-crystallins. The thermal stability was determined by time-dependent change in light scattering as monitored at 360 nm at 65°C. By 12 minutes of incubation under this condition, the D140N mutant αB-crystallin began to aggregate. In contrast, wild-type αB-crystallin remained soluble up to 120 minutes. When mixed with mutant αB-crystallin at 1:1 (wt:wt) ratio, wild-type αB-crystallin could not prevent the aggregation of mutant αB-crystallin.

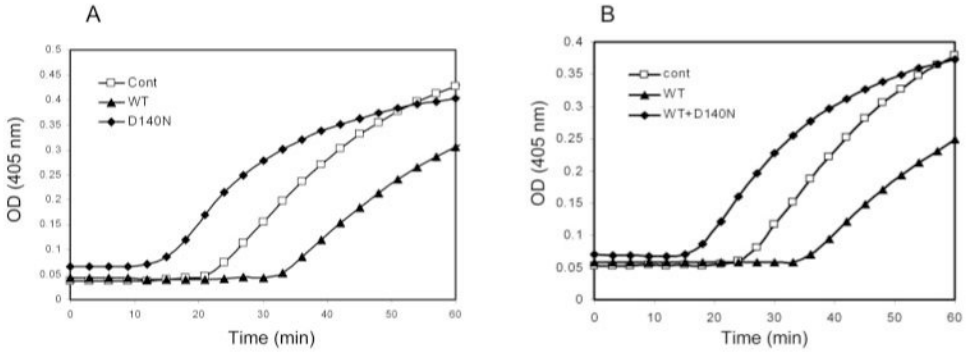

FIGURE 9.

Chaperone-like activity of wild-type and D140N mutant *α*B-crystallins. The chaperone-like activity was evaluated by prevention of DTT-induced aggregation of insulin at room temperature. Wild-type *α*B-crystallin with a 1:1 (wt/wt) ratio to insulin significantly inhibited DTT-induced aggregation of insulin. In contrast, D140N mutant *α*B-crystallin at the same ratio promoted, rather than inhibited, the aggregation of reduced insulin (**A**). Moreover, chaperone-like activity of wild-type *α*B-crystallin was compromised when 1:1 (wt/wt) mixed with D140N mutant *α*B-crystallin (**B**).

TABLE 1

Clinical Data of the ADCC Pedigree

Affected Individual	Age (y)	Age at Onset (y)	Best Corrected Visual Acuity before Sugery	Type of Cataract	Age at Surgery (y)	Surgery	Complications
I:1		3	Not available	Not available		None	
II:1		1	Not available	Not available		None	
II:2		1	Not available	Not available		None	
II:3	60	1	Not available	Not available		None	
III:1	65	1	Not available	Lamellar		None	
III:2	63	1	Not available	Lamellar		None	
III:3	52	3	0.1 OU	Lamellar	52	Phaco+IOL	None
III:7	40	1	Not available	Lamellar	39	Phaco+IOL	None
III:8	38	1	Not available	Lamellar	36	Phaco+IOL	None
IV:1	24	1	0.3 OU	Lamellar	24	Phaco+IOL	None
IV:2	22	1	0.2 OU	Lamellar	22	Phaco+IOL	None
V:1	3	1	0.2 OU	Lamellar	3	IA+IOL	PCO

Phaco+IOL, cataract surgery of phacoemulsification with intraocular lens implantation; IA+IOL, irrigation and aspiration of cataract with intraocular lens implantation; PCO, posterior capsular opacification.